THE JOURNAL OF BIOLOGICAL CHEMISTRY VOL. 286, NO. 31, pp. 27781–27791, August 5, 2011

Transport Activity of the High-affinity Monocarboxylate Transporter MCT2 Is Enhanced by Extracellular Carbonic Anhydrase IV but Not by Intracellular Carbonic Anhydrase II*

Received for publication, April 27, 2011, and in revised form, June 7, 2011 Published, JBC Papers in Press, June 16, 2011, DOI 10.1074/jbc.M111.255331

Michael Klier[‡§], Christina Schüler[‡], Andrew P. Halestrap[¶], William S. Sly[‖], Joachim W. Deitmer[‡], and Holger M. Becker[§1]

From the [‡]Abteilung für Allgemeine Zoologie, and [§]Arbeitsgruppe Zoologie/Membrantransport, Fachbereich Biologie, Technische Universität Kaiserslautern, P. O. Box 3049, 67653 Kaiserslautern, Germany, the [¶]Department of Biochemistry, University of Bristol, School of Medical Sciences, University Walk, Bristol BS8 1TD, United Kingdom, and the [‖]Edward A. Doisy Department of Biochemistry and Molecular Biology, Saint Louis University School of Medicine, St. Louis, Missouri 63104

The ubiquitous enzyme carbonic anhydrase isoform II (CAII) has been shown to enhance transport activity of the proton-coupled monocarboxylate transporters MCT1 and MCT4 in a non-catalytic manner. In this study, we investigated the role of cytosolic CAII and of the extracellular, membrane-bound CA isoform IV (CAIV) on the lactate transport activity of the high-affinity monocarboxylate transporter MCT2, heterologously expressed in *Xenopus* oocytes. In contrast to MCT1 and MCT4, transport activity of MCT2 was not altered by CAII. However, coexpression of CAIV with MCT2 resulted in a significant increase in MCT2 transport activity when the transporter was coexpressed with its associated ancillary protein GP70 (embigin). The CAIV-mediated augmentation of MCT2 activity was independent of the catalytic activity of the enzyme, as application of the CA-inhibitor ethoxyzolamide or coexpressing the catalytically inactive mutant CAIV-V165Y did not suppress CAIV-mediated augmentation of MCT2 transport activity. Furthermore, exchange of His-88, mediating an intramolecular H^+-shuttle in CAIV, to alanine resulted only in a slight decrease in CAIV-mediated augmentation of MCT2 activity. The data suggest that extracellular membrane-bound CAIV, but not cytosolic CAII, augments transport activity of MCT2 in a non-catalytic manner, possibly by facilitating a proton pathway other than His-88.

High-energy metabolites, such as lactate, pyruvate, and ketone bodies, are transported into and out of cells via monocarboxylate transporters (MCT[2], SLC16), of which 14 isoforms have been described (1). MCT isoforms 1–4 have been reported to transport monocarboxylates in an electroneutral transport mode of 1 proton:1 monocarboxylate with different substrate affinities. With a K_m value of ~0.7 mM, MCT isoform 2 (MCT2) has the highest affinity for lactate among all the MCTs (2). MCT2 is primarily found in liver, kidney, testis, and in the brain (3, 4). In liver and kidney, MCT2 facilitates the uptake of lactate, in part for glyconeogenesis (5). In the brain, MCT2 is exclusively expressed in neurons, where it facilitates the import of lactate, which is exported from astrocytes via MCT1 and MCT4 (6–8). Experiments using heterologous protein expression in *Xenopus* oocytes revealed that MCTs require an ancillary protein, either CD147 (basigin, extracellular matrix metalloproteinase inducer) or GP70, for proper expression in the plasma membrane and, hence, transport activity. Although MCT1, MCT3, and MCT4 are normally associated with CD147, which is intrinsically expressed in *Xenopus* oocytes, MCT2 prefers GP70, which is not found in frog oocytes (9, 10).

Mammalian carbonic anhydrases (CA), included in the α-class of CAs, of which 16 isoforms are identified, are mostly monomeric zinc-metalloenzymes with a molecular mass of around 30 kDa that catalyze the reversible hydration of CO_2 to HCO_3^- and H^+ (11). In this study, we used the two isoforms, CAII and CAIV. CAII is found in the cytosol, whereas CAIV is linked to the extracellular surface of the cell membrane via a glycosyl-phosphatidyl-inositol anchor (12).

In the brain, CAII is highly expressed in the cytosol of oligodendrocytes and astrocytes, where it plays a supportive role in pH regulation (13, 14), but expression is low in neurons. CAIV, on the other hand, is expressed at the surface of neurons and astrocytes, where it catalyzes buffering of brain extracellular fluid (15) and facilitates lactate transport (16).

Both the intracellular isoform CAII and the extracellular CAIV have been found to interact with different acid/base transporting proteins. *In vitro* studies and experiments using heterologous protein expression revealed that CAII binds to, and enhances the activity of, the chloride/bicarbonate exchanger AE1 (17, 18), the sodium bicarbonate cotransporter NBCe1 (19, 20), the sodium/hydrogen exchanger NHE1 (21), and the monocarboxylate transporters 1 and 4 (22–26). In addition, it has been shown in muscle cells that coexpression of CAII with acid/base transporting proteins like NBC, NHE1, and also the MCTs, greatly supports acid/base homeostasis (27).

Besides CAII, extracellular CAIV has also been shown to interact with NBCe1 (17, 28) and AE1 (17, 29). In addition, it

* The work was funded by the Deutsche Forschungsgemeinschaft Grant DE 231/24-1 (to J. W. D.) and by the Landesschwerpunkt Membrantransport (to H. B. and J. W. D.).

[1] To whom correspondence should be addressed: Arbeitsgruppe Zoologie/Membrantransport, FB Biologie, TU Kaiserslautern, P. O. Box 3049, 67653 Kaiserslautern, Germany. Tel.: 49-0-631-205-2491; Fax: 49-0-631-205-3515; E-mail: h.becker@biologie.uni-kl.de.

[2] The abbreviations used are: MCT, monocarboxylate transporter; CA, carbonic anhydrase(s); pH_i, intracellular pH; EZA, 6-Ethoxy-2-benzothiazolesulfonamide.

has been demonstrated that extracellular carbonic anhydrase activity facilitates lactate transport and work capacity in skeletal muscle (30–32).

We have shown recently that CAII can enhance transport activity of MCT1 and MCT4, heterologously expressed in *Xenopus* oocytes, in a non-catalytic manner, presumably by dissipating intracellular proton microdomains via an intramolecular proton shuttle (22–26). In this study, we have tested whether intracellular CAII or extracellular CAIV can increase transport activity of MCT2 when heterologously coexpressed in *Xenopus* oocytes. Our studies revealed that MCT2 transport activity, in contrast to transport via MCT1 and MCT4, is not enhanced by CAII. However, coexpression of MCT2 with CAIV resulted in a robust increase in MCT2 transport activity that was independent of the catalytic activity of the enzyme.

EXPERIMENTAL PROCEDURES

Constructs, Oocytes, and Injection of cRNA and Protein—The mutant CAIV-H88A was generated by PCR using the plasmid vector pGEM-He-Juel, containing the human hCAIV coding region and mismatched primers. Primers containing the desired mutation had the sequence 5′-GGACTGTCCAAAATAACGGGGCATCAGTGATG-3′ (forward) and 5′-CATCACTGATGCCCCGTTATTTTGGACAGTCC-3′ (reverse). The resulting vector DNA containing the human hCAIV coding region with the desired mutation was transformed into *Escherichia coli* XL1-Blue supercompetent cells for amplification. Mutation of CAIV was confirmed by sequencing (SEQ-IT GmbH, Kaiserslautern, Germany).

Human CAII-WT, CAIV-WT, CAIV-V165Y, CAIV-H88A, and rat GP70 were subcloned into the oocyte expression vector pGEM-He-Juel, which contains the 5′ and the 3′ untranscribed regions of the *Xenopus* β-globin flanking the multiple cloning site. Rat MCT2-cDNA cloned into the oocyte expression vector pGEM-He-Juel was kindly provided by Dr. Stefan Bröer, Canberra, Australia (2, 4). Plasmid DNA was transcribed *in vitro* with T7 RNA polymerase (mMessage mMachine, Ambion, Inc., Austin, TX) as described earlier (33). *Xenopus laevis* females were purchased from *Xenopus* Express, Vernassal, France. Segments of ovarian lobules were surgically removed under sterile conditions from frogs anesthetized with 1 g/liter of 3-amino-benzoic acid ethylester (MS-222, Sigma-Aldrich) and rendered hypothermic. The procedure was approved by the Landesuntersuchungsamt Rheinland-Pfalz, Koblenz. As described earlier (33), oocytes were singularized by collagenase (Collagenase A, Roche) treatment in Ca^{2+}-free oocyte saline (pH 7.8) at 28 °C for 2 h. The singularized oocytes were left overnight in an incubator at 18 °C in Ca^{2+}-containing oocyte saline (pH 7.8) to recover. Oocytes of the stages V and VI were injected with 5 ng of cRNA coding for MCT2, either together with 10 ng of cRNA coding for GP70 or alone, dissolved in diethyl pyrocarbonate-H_2O. Measurements were carried out 3 to 6 days after injection of cRNA. CAII and CAIV were either injected as protein or coexpressed with the MCT2. For injection of protein, 50 ng of CAII, isolated from bovine erythrocytes (C3934, Sigma-Aldrich), or 35 ng of CAIV, isolated from secretion medium of CHO cells expressing recombinant proteins, dissolved in 27.6 nl DEPC-H_2O, were injected 12–24 h before electrophysiological measurements. For expression of CAII-WT, 12 ng cRNA coding for CAII-WT were injected. For expression of CAIV-WT or one of the CAIV mutants, CAIV-V165Y and CAIV-H88A, each oocyte was injected with 2 ng of the corresponding cRNA. The oocyte saline had the following composition: 82.5 mM NaCl, 2.5 mM KCl, 1 mM $CaCl_2$, 1 mM $MgCl_2$, 1 mM Na_2HPO_4, 5 mM HEPES titrated with NaOH to pH 7.0. In lactate-containing saline, NaCl was replaced by an equivalent amount of Na-L-lactate. In the bicarbonate-containing saline, NaCl was replaced by an equivalent amount of $NaHCO_3$, and the solution was aerated with 2% CO_2/98% O_2 or 5% CO_2/95% O_2. Application of lactate was carried out in HEPES-buffered solution at pH 7.0 unless stated otherwise, in the nominal absence of CO_2/ HCO_3^-, containing approximately 0.008 mM of CO_2 from air and hence a HCO_3^- concentration of less than 0.2 mM.

Immunohistochemical Analysis of MCT2 and CAIV—Frog oocytes, either injected with 5 ng cRNA for MCT2 alone or together with 10 ng cRNA for GP70, as well as native control oocytes were fixed in 4% paraformaldehyde in PBS (Roti-Histofix 4%, Roth, Karlsruhe, Germany) 4 days after cRNA injection. Oocytes were treated with 100% methanol and permeabilized with 0.1% Triton X-100 (Sigma-Aldrich). Unspecific binding sites were blocked with 3% BSA (Sigma-Aldrich), 1% normal goat serum (Sigma-Aldrich) and 1% normal donkey serum (Sigma-Aldrich). Afterward, oocytes were embedded in 2.5% agarose (peqGOLD low-melt-agarose, peqlab, Erlangen, Germany) and sectioned into 100-μm thick slices with a microtome (752 M Vibroslice, Campden Instruments Ltd., Loughborough, UK). Slices were incubated in PBS containing the primary antibody against MCT2 (1:200; chicken anti-MCT2 polyclonal antibody, Millipore, Temecula, CA) overnight at 4 °C. Sectioned oocytes were then incubated in PBS with the secondary antibody (1:100; Alexa Fluor 488 goat anti-chicken IgG, Invitrogen).

To determine the localization of CAIV, oocytes expressing CAIV (2 ng RNA) or injected with 35 ng CAIV as well as native control oocytes were fixed for 20 min in 4% paraformaldehyde in PBS. One batch of oocytes was permeabilized with 100% methanol and Triton X-100, the other batch was not permeabilized to allow an exclusive detection of extracellularly expressed proteins. Unspecific binding sites were blocked with 3% BSA and 1% normal goat serum. Anti-hCAIV mouse monoclonal antibody (R&D Systems GmbH, Wiesbaden-Nordenstadt, Germany) diluted 1:25 in 1% BSA with or without 0.01% Triton X-100 was used for detection of CAIV. Oocytes were then incubated with the secondary antibody (1:100, Alexa Fluor 488 goat anti-mouse IgG, Invitrogen).

The sections stained against MCT2 or oocytes stained against CAIV were analyzed with a confocal laser-scanning microscope (LSM 700, Carl Zeiss GmbH, Oberkochen, Germany).

Determination of CA Activity—Activity of CA was determined by monitoring the ^{18}O depletion of doubly labeled $^{13}C^{18}O_2$ through several hydration and dehydration steps of CO_2 and HCO_3^- at 25 °C (34, 35). The reaction sequence of ^{18}O loss from $^{13}C^{18}O^{18}O$ ($m/z = 49$) over the intermediate product $^{13}C^{18}O^{16}O$ ($m/z = 47$) and the end product $^{13}C^{16}O^{16}O$ ($m/z =$

45) was monitored with a quadropole mass spectrometer (OmniStar GSD 320, Pfeiffer Vacuum, Asslar, Germany). The relative ^{18}O enrichment was calculated from the measured 45, 47, and 49 abundance as a function of time according to log enrichment = log (49 × 100/(49 + 47 + 45)). For the calculation of CA activity, the rate of ^{18}O degradation was obtained from the linear slope of the log enrichment over the time, using the spreadsheet analyzing software OriginPro 7 (OriginLab Corp. Northampton, MA). The rate was compared with the corresponding rate of the non-catalyzed reaction. Enzyme activity in units (U) was calculated from these two values as defined by Badger and Price (36). From this definition, one unit corresponds to 100% stimulation of the non-catalyzed ^{18}O depletion of doubly labeled $^{13}C^{18}O_2$. For the experiments, the cuvette was filled with 6 ml of oocyte saline with a pH of 7.0. After addition of $^{13}C^{18}O_2$, the spontaneous degradation was measured for 5 min. Batches of 20 oocytes expressing MCT2, GP70, and CAIV-WT or mutants of CAIV, respectively, were lysed in 80 μl of oocyte saline, pipetted into the cuvette, and the catalyzed degradation was determined for 10 min. For calibration, purified CAIV was added directly as protein, yielding a final concentration of 0.25, 0.5, 1, and 2 μg, respectively.

Western Blot Analysis—For comparison of protein levels of expressed MCT2 and CAIV, Western blot analyses were performed. For each sample, 20 oocytes were lysed by sonication in 2% sodium dodecylsulfate solution with protease inhibitor (Complete Mini EDTA-free, Roche) 4 days after injection of cRNA. Total protein content was determined using a BCA protein assay kit (Pierce, Fisher Scientific GmbH). Extracts containing 20 μg or 50 μg of protein per sample for detection of MCT2 or CAIV, respectively, were separated by 4–12% SDS-PAGE and transferred to nitrocellulose membranes. Proteins of interest were detected by antibody staining. For detection of MCT2 anti-MCT2 (D-5) mouse monoclonal antibody (diluted 1:200, Santa Cruz Biotechnology, Inc., Heidelberg, Germany) was used, and for detection of CAIV, anti-hCAIV mouse monoclonal antibody (diluted 1:300, R&D Systems GmbH) was used. As a loading control, β-tubulin was labeled with anti-β-tubulin mouse monoclonal antibody (diluted 1:1000, Sigma Aldrich). Primary antibodies were labeled with goat anti-mouse IgG horseradish peroxidase-conjugated secondary antibody (diluted 1:4000, Santa Cruz Biotechnology, Inc.). Membranes were analyzed after incubation with Lumi-Light Western blotting substrate (Roche) with a Versa Doc imaging system (Bio-Rad). Quantification of proteins was carried out with the software Quantity One 4.5 (Bio-Rad). For each protein band, the pixel density per square millimeter was calculated and background pixel density subtracted. To allow comparison of different Western blots, all measured protein concentrations on one blot were normalized to the concentration of one protein on the same blot.

Biotinylation—Localization of CAIV was investigated by biotinylation of extracellular proteins with Pierce Cell Surface Protein Isolation Kit (Thermo Fisher Scientific, Inc.). Four days after injection of cRNA, 50 CAIV-expressing or native oocytes were incubated in membrane-impermeable EZ-Link Sulfo-NHS-SS-Biotin (1 mg/ml PBS, 30 min, 4 °C). After the incubation period, quenching solution was added to the oocytes to stop the reaction (30 min, 4 °C), before washing them three times in Tris-buffered solution. Oocytes were lysed by sonication and incubation in 400 μl of lysis buffer with protease inhibitor (Complete Mini EDTA-free, Roche). Oocyte lysate was then applied on a column filled with 300 μl NeutrAvidin-agarose suspension and incubated for 1 h at room temperature on an overhead shaker before centrifugation and four times washing with wash buffer. Elution was carried out by incubation of the NeutrAvidin-agarose resin in 120 μl SDS-PAGE sample buffer containing 50 mM dithiothreitol for 15 min at room temperature on an overhead shaker before heating the sample for 5 min at 95 °C. Each 25 μl of the eluates of CAIV-expressing and native oocytes as well as 0.1 μg of hCAIV protein were separated by SDS-PAGE. Detection of CAIV in Western blot analysis was performed as described above.

Intracellular pH Measurements—For measurement of intracellular pH (pH_i) and membrane potential, double-barrelled microelectrodes were used. The manufacture and application have been described in detail previously (33, 37). For calibration, electrodes were perfused with HEPES-buffered oocyte saline (pH 7.0). After a stable electrode potential was reached, oocyte saline (pH 6.4), was applied until the electrode again reached a stable potential.

As described previously (38), optimal intracellular pH changes were detected when the electrode was located near the inner surface of the plasma membrane. All experiments were carried out at room temperature.

Extracellular pH Surface Measurements—Electrodes were manufactured and calibrated in the same way as described for intracellular pH measurements. Instead of impaling the double-barreled microelectrode, its tip was gently pushed against the outer surface of the oocyte. Oocytes were clamped to a membrane potential of −40 mV using two additional KCl electrodes. Under these conditions, the reference channel of the extracellular pH-sensitive electrode displayed a reference potential between 0 and −5 mV.

Calculation of $[H^+]_i$—The measurements of pH_i were stored digitally using homemade PC software based on the program LabView (National Instruments Germany GmbH, München, Germany) and were routinely converted into intracellular H^+ concentration, $[H^+]_i$. This should provide changes in the $[H^+]_i$ that take into account the different pH baseline, as *e.g.* measured in HEPES- and CO_2/ HCO_3^--buffered salines (33). The rate of change of the measured $[H^+]_i$ was analyzed by determining the slope of a linear regression fit using the spread sheet program OriginPro 7. Extracellular pH measurements were presented as pH values.

Buffer Capacity and Proton Fluxes—The intrinsic buffering power β_i was calculated from the maximal "instantaneous" pH_i changes recorded when changing from HEPES- to CO_2/ HCO_3^--buffered saline. The CO_2-dependent buffering power, β_{CO2}, was calculated from the intracellular bicarbonate concentration in the oocytes ($\beta_{CO2} = 2.3 \cdot [HCO_3^-]$), and the bicarbonate concentration was obtained from the Henderson-Hasselbalch equation, assuming a $[CO_2]$ of 0.00835 mM in the HEPES-buffered, nominal CO_2-free solution. The total buffer capacity, β_t, was defined as the sum of β_i and β_{CO2}.

Net H^+ flux J_H (mM/min), defined as the net transport of acid and/or base equivalents across the cell membrane, was calculated as the product of the rate of pH_i change, $\Delta pH_i/t$, and the total buffer capacity β_t (33).

Voltage-clamp Recording—A borosilicate glass capillary, 1.5 mm in diameter, was pulled to a micropipette and backfilled with 3 M KCl. For voltage-clamp, this electrode was used for current injection and was connected to the head-stage of an Axoclamp 2B amplifier (Axon Instruments). The actual membrane voltage was recorded by the reference barrel of the double-barreled pH-sensitive microelectrode. Oocytes were clamped to a holding potential of −40 mV.

Calculation and Statistics—Statistical values are presented as means ± S.E. of the mean. For calculation of significance in differences, Student's *t* test or, if possible, a paired *t* test was used. In the figures shown, a significance level of $p \leq 0.05$ is marked with *, $p \leq 0.01$ with **, and $p \leq 0.001$ with ***.

RESULTS

GP70 Is Required for Efficient Expression of MCT2 in Xenopus Oocytes—It has been shown that functional expression of MCT2 requires the ancillary protein GP70, which is not endogenously expressed in *Xenopus* oocytes (9, 10). To examine the need of GP70 for proper expression of MCT2, we either expressed MCT2 alone or together with GP70 in *Xenopus* oocytes. Oocytes expressing GP70 alone and native oocytes were used as negative control. Activity of MCT2 was tested by application of 0.3, 1, and 5 mM lactate, and the lactate-induced increase in intracellular H^+ concentration was determined with pH-sensitive microelectrodes (Fig. 1*A*). Coexpression of GP70 with MCT2 induced a significant increase both in the rate of rise (Fig. 1*B*) and in the amplitude (*C*) of lactate-induced acidification, in line with a significant increase in functional MCT2 expression and activity when the transporter is coexpressed with its ancillary protein GP70. In native and only GP70-expressing oocytes, respectively, application of lactate induced no change in intracellular H^+ concentration (Fig. 1*A*). Therefore the lactate-induced changes in intracellular H^+ concentration in MCT2-expressing oocytes are attributed to transport activity of MCT2. Integration of MCT2 into the oocyte plasma membrane was further evaluated via antibody staining using confocal laser scanning microscopy (Fig. 1*D*). The staining reveals a sharp signal for MCT2 in the plasma membrane when it is coexpressed with GP70, whereas expression of MCT2 alone results in a diffuse signal for the transporter, both at the cell membrane and in the cytosol. These results support the conclusion that incorporation of MCT2 into the plasma membrane of the oocyte is facilitated by GP70.

Activity of MCT2 Is Not Enhanced by CAII—It has previously been shown that injected or coexpressed CAII can enhance transport activity of MCT1 and 4 when heterologously expressed in *Xenopus* oocytes (22–26). Injection of 50 ng of CAII into oocytes coexpressing MCT2+GP70 resulted in no significant increase in the rate of rise of lactate-induced acidification (Fig. 2, *A* and *B*), indicating no functional interaction between MCT2 and CAII. Injected CAII displayed significant catalytic activity in the oocyte, as indicated by the rate of rise in intracellular H^+ concentration, induced by application of 5% CO_2/10 mM HCO_3^-, which was increased 2.8-fold in CAII-injected oocytes compared with oocytes expressing MCT2 alone (Fig. 2*C*). When CAII was coexpressed with MCT2 and GP70 in oocytes, lactate-induced acidification was the same as without coexpressed CAII (not shown).

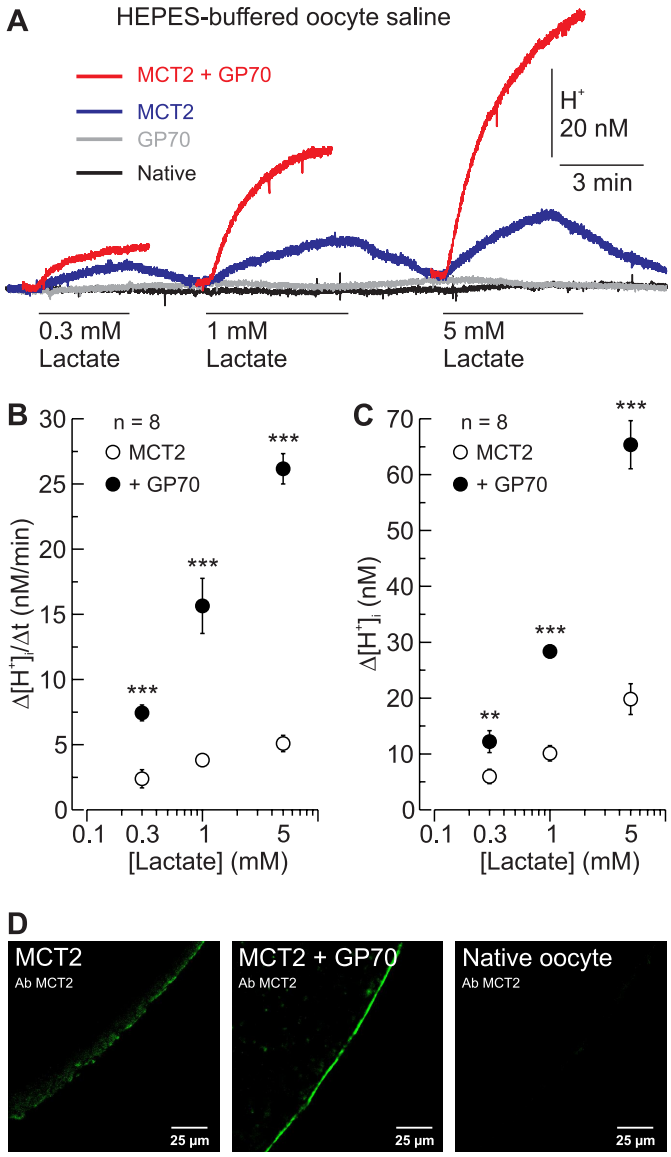

FIGURE 1. **MCT2 needs GP70 for robust expression and function in *Xenopus* oocytes.** *A*, original recordings of $[H^+]_i$ concentration in *Xenopus* oocytes either expressing MCT2 alone (*blue trace*), MCT2+GP70 (*red trace*), GP70 alone (*gray trace*), or native oocytes (*black trace*) during application of 0.3, 1, and 5 mM lactate. Rate of change (*B*) and amplitude (*C*) in $[H^+]_i$ induced by application of lactate in oocytes expressing MCT2 (○) and MCT2+GP70 (●), respectively. The *asterisks* at the circles for MCT2+GP70-coexpressing oocytes refer to the values of MCT2-expressing cells. *D*, fluorescence staining of MCT2 in slices of oocytes expressing MCT2 alone (*left panel*) and MCT2+GP70 (*middle panel*), respectively. Native oocytes were stained against MCT2 as control (*right panel*). A significance level of $p < 0.01$ is marked with **, and $p < 0.001$ with ***.

Transport Activity of MCT2 Is Enhanced by CAIV in a Non-catalytic Manner—To test a possible effect of the extracellular, membrane-bound CAIV on transport activity of MCT2, we coexpressed CAIV together with MCT2 and GP70. Transport activity of MCT2 was determined by application of 1 and 5 mM lactate in the nominal absence and in the presence of 2% CO_2/4

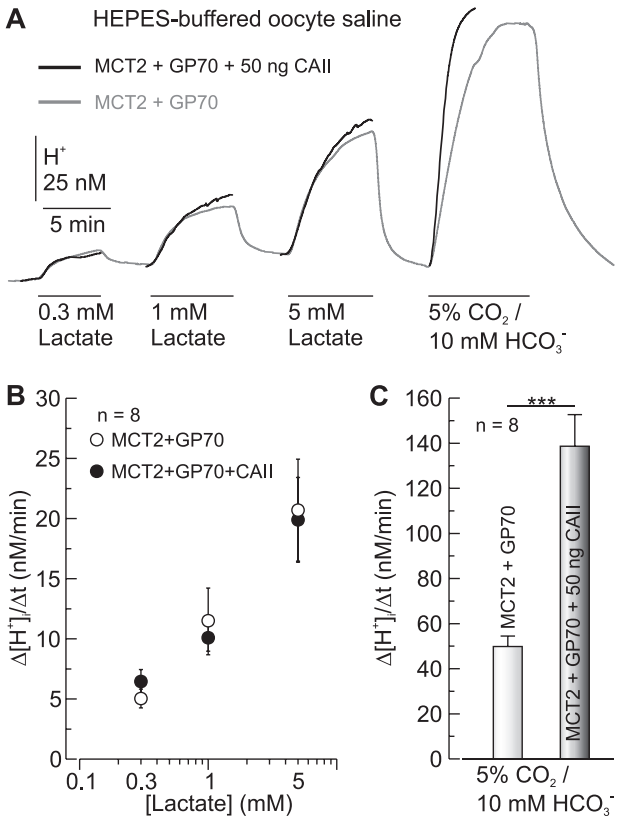

FIGURE 2. **CAII does not enhance activity of MCT2.** *A*, original recordings of $[H^+]_i$ in MCT2+GP70-coexpressing *Xenopus* oocytes either injected with 50 ng of CAII protein (*black trace*) or 27.6 nl of H_2O as control (*gray trace*) during application of 0.3, 1, and 5 mM lactate and 5% CO_2/10 mM HCO_3^-. Shown is the rate of change in $[H^+]_i$ in MCT2+GP70-coexpressing oocytes injected with 50 ng CAII or water, as induced by application of lactate (*B*) and CO_2/ HCO_3^- (*C*), respectively. A significance level of $p < 0.001$ is marked with ***.

mM HCO_3^- (pH 7.0) before and during application of 10 μM of the CA inhibitor 6-Ethoxy-2-benzothiazolesulfonamide (EZA) (Fig. 3*A*). Both in the absence and in the presence of CO_2/ HCO_3^-, coexpression of CAIV with MCT2 and GP70 induced a ~2.5-fold increase in MCT2 activity, as determined from the rate of rise in lactate-induced acidification (Fig. 3, *B* and *C*). In both cases, CAIV-induced increase in MCT2 activity was insensitive to the inhibition of CAIV activity by EZA (Fig. 3, *A–C*). Inhibition of CAIV catalytic activity by 10 μM EZA was confirmed by application of CO_2/ HCO_3^- (Fig. 3*D*). The rate of CO_2-induced acidification was increased by a factor of 5.4 in CAIV-expressing oocytes as compared with non-CA-expressing cells. In the presence of EZA, no difference between CAIV-expressing and non-CAIV-expressing oocytes was observed.

It has previously been shown that carbonic anhydrases can influence intracellular buffer capacity (39, 40). Therefore, we determined cytosolic buffer capacity of the oocyte via application of CO_2 in the absence and presence of EZA (Fig. 3*E*). The data indicated no change in intrinsic or in CO_2/ HCO_3^--dependent buffer capacity when CAIV was expressed in oocytes, with a value of 22–24 mM total cytosolic buffer capacity.

With the buffer capacity known, lactate-induced acid/base flux could be calculated from the rate of change in intracellular pH. As already demonstrated for the lactate-induced change in proton concentration, coexpression of MCT2 and GP70 with CAIV induced a significant increase in acid/base flux by a factor of ~2.9, both in the nominal absence and in the presence of CO_2/ HCO_3^- (Fig. 3, *F* and *G*). Furthermore, the CAIV-induced increase in acid/base flux was insensitive to CA inhibition by EZA. The data indicate that CAIV, heterologously expressed in *Xenopus* oocytes, increases transport activity of MCT2 in a non-catalytic manner.

Mechanism of CAIV-mediated Increase in MCT2 Transport Activity—To further investigate the role of CAIV catalytic activity and its intramolecular proton shuttle on MCT2 activity, we applied two mutants of CAIV, the catalytically inactive mutant CAIV-V165Y and CAIV-H88A, a mutant with an impaired proton shuttle (analogous to the H64A mutant of CAII).

To test the influence of these mutants on MCT2 transport activity, we coexpressed MCT2 and GP70 either with CAIV-V165Y, with CAIV-H88A, or with CAIV-WT as a control. Both mutants induced a significant increase in the rate of lactate-induced acidification, although CAIV-H88A imposed a significantly lower increase by about 25% in MCT2-mediated acidification than CAIV-WT (Fig. 4*A*).

Catalytic activity of the CAIV mutants in intact oocytes was determined by the rate of intracellular acidification during application of CO_2. CAIV-H88A displayed notable but, compared with CAIV-WT, significantly reduced catalytic activity, whereas CAIV-V165Y showed no catalytic activity at all (Fig. 4*B*). Both CAIV-WT and CAIV-H88A were inhibited by application of 10 μm EZA.

Potential changes in MCT2 expression level because of coexpression of MCT2 with CAIV were checked by quantifying the amount of MCT2 in oocytes either expressing MCT2 alone or oocytes coexpressing MCT2, GP70, and CAIV-WT or CAIV mutants relative to the expression of MCT2 in oocytes injected with RNA for MCT2 and GP70 alone (Fig. 5, *A* and *C*). β-Tubulin was used as a loading control (Fig. 5*B*). The data revealed that neither coexpression of CAIV-WT nor that of the two CAIV mutants alter the expression level of MCT2. In contrast, oocytes injected with RNA for MCT2 alone without GP70 express only 20% of MCT2 of that expressed with GP70, whereas the values for the β-tubulin did not show differences to GP70-coexpressing oocytes.

The expression levels of the CAIV mutants, relative to the expression of CAIV-WT, were checked by relative quantification of CAIV in oocytes coexpressing MCT2 and GP70 either with CAIV-WT or one of the two CAIV mutants (Fig. 5*D*) and β-tubulin as loading control (*E*). The data revealed no significant difference in the relative expression level of CAIV-WT and the mutants (Fig. 5*F*).

The catalytic activity of the two mutants and CAIV-WT was also determined *in vitro* by mass spectrometrical analysis. Twenty oocytes expressing CAIV-WT showed a catalytic activity of 8.2 units/ml, whereas oocytes expressing CAIV-V165Y displayed no increase in activity as compared with native cells (Fig. 6, *A* and *B*). The catalytic activity of the mutant CAIV-H88A was decreased to 72% of the activity of CAIV-WT. Coexpression of MCT2 and GP70 induced no significant change in catalytic activity as compared with native oocytes, whereas the triple expression of MCT2, GP70, and CAIV-WT led to a

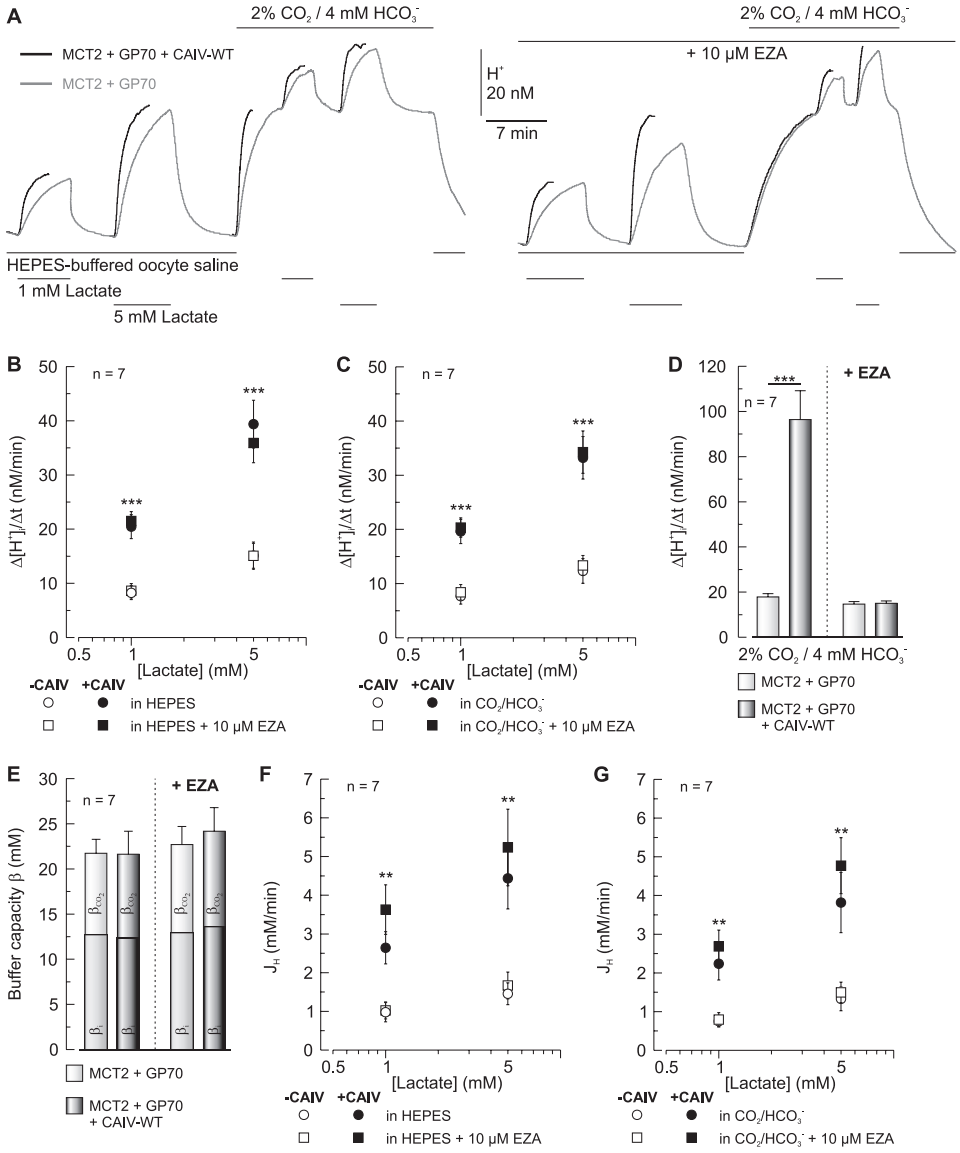

FIGURE 3. **Transport activity of MCT2 is enhanced by CAIV.** *A*, original recordings of $[H^+]_i$ in *Xenopus* oocytes, either coexpressing MCT2+GP70 (*gray trace*) or MCT2+GP70+CAIV (*black trace*) during application of 1 and 5 mM lactate, in the absence and presence 2% CO_2/4 mM HCO_3^- (at constant pH_e of 7.0), before and during application of 10 μM EZA. Shown is the rate of change in $[H^+]_i$ in oocytes coexpressing MCT2+GP70 (○ and □) and MCT2+GP70+CAIV (● and ■), respectively, as induced by application of lactate in the absence (*B*) and presence (*C*) of CO_2/ HCO_3^- and by application of CO_2/ HCO_3^- itself (*D*) before (○ and ●) and during application of EZA (□ and ■). *E*, intrinsic (β_i) and CO_2/ HCO_3^--dependent (β_{CO2}) buffer capacity in oocytes coexpressing MCT2+GP70 and MCT2+GP70+CAIV, and in the absence and presence of EZA, respectively. Shown also is the lactate-induced acid/base flux in oocytes coexpressing MCT2+GP70 (○ and □) and MCT2+GP70+CAIV (□ and ■), respectively, in the absence (*F*) and presence (*G*) of CO_2/ HCO_3^-, with (□ and ■) and without EZA (○ and ●). The *asterisks* at the symbols for MCT2+GP70+CAIV-coexpressing oocytes refer to the values of MCT2+GP70-coexpressing cells. A significance level of $p < 0.01$ is marked with **, and $p < 0.001$ with ***.

significant increase in catalytic activity. To determine the amount of CAIV expressed in the oocytes, CA activity was calibrated by measuring the enzymatic activity of defined amounts of CAIV protein (0.25, 0.5, 1, and 2 μg) to generate a calibration curve (Fig. 6*C*). Calculating the amount of active CA in the oocytes revealed that expression of CAIV was reduced to 39% when the enzyme was coexpressed with MCT2 and GP70 (Fig. 6*D*).

Localization of CAIV—Localization of CAIV at the oocyte plasma membrane was determined by measurements of extracellular surface pH using pH-sensitive microelectrodes positioned on the outer membrane surface (Fig. 7*A*). In native oocytes, changing from a HEPES-buffered to a 5% CO_2/10 mM HCO_3^--buffered solution at constant pH 7.0 induced a small transient extracellular alkalinization, whereas removal of CO_2/ HCO_3^- induced a small transient acidification. However, expression of CAIV resulted in an EZA-sensitive increase of these transients by a factor of 2.7 for the CO_2-induced alkalinization ($p \leq 0.001$) and by a factor of 4.0 for the acidification induced by withdrawal of CO_2 ($p \leq 0.001$, Fig. 7*B*). In contrast to CAIV, intracellular CAII induced no increase in the transients compared with native oocytes. These results indicate extracellular CA activity because of the localization of CAIV at the outer face of the cell membrane. This extracellular localization of CAIV was confirmed by biotinylation of CAIV (Fig. 7*C*) and by antibody staining of expressed and injected CAIV in

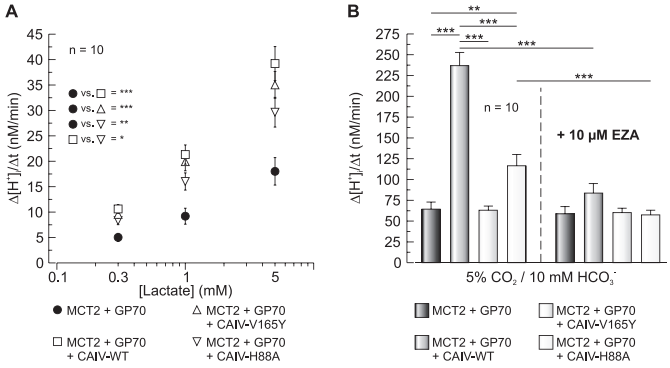

FIGURE 4. **Activity of MCT2 is also enhanced by the catalytically inactive mutant CAIV-V165Y and by CAIV-H88A, a mutant with impaired H^+ shuttle.** Rate of rise in $[H^+]_i$, as induced by application of 0.3, 1, and 5 mM lactate (*A*) and 5% CO_2/10 mM HCO_3^- (*B*) in oocytes coexpressing MCT2+GP70 (● in *A*), MCT2+GP70+CAIV-WT (□ in *A*), MCT2+GP70+CAIV-V165Y (△ in *A*), and MCT2+GP70+CAIV-H88A (▽ in *A*), respectively. A significance level of $p <$ 0.05 is marked with *, $p < 0.01$ with **, and $p < 0.001$ with ***.

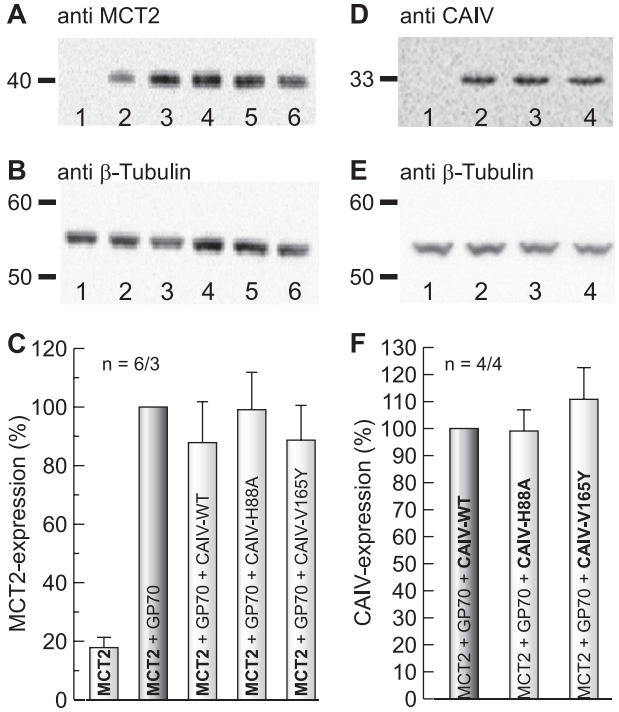

FIGURE 5. **Expression levels of MCT2 are increased by coexpression with GP70 but not by coexpression with CAIV.** Western blot analysis for MCT2 (*A*) and CAIV (*D*), respectively, and β-tubulin (*B* and *E*) as loading control from native oocytes (*A1* and *D1*) and oocytes expressing MCT2 (*A2*), MCT2+GP70 (*A3*), MCT2+GP70+CAIV-WT (*A4* and *D2*), MCT2+GP70+CAIV-H88A (*A5* and *D3*), and MCT2+GP70+CAIV-V165Y (*A6* and *D4*). Quantification of the relative expression levels of MCT2 (*C*) and CAIV (*F*), respectively, by Western blot analyses. The *n* value is given as blots/badges of oocytes. The expression level of MCT2 in non-GP70-expressing oocytes is significantly lower ($p \leq 0.001$) as compared with GP70-expressing cells, which do not differ significantly from each other. The expression levels of CAIV mutants do not differ from CAIV-WT.

permeabilized and non-permeabilized oocytes (Fig. 7, *D* and *E*). CAIV, expressed in oocytes injected with 2 ng of CAIV-cRNA, could be detected in both permeabilized and non-permeabilized oocytes, indicating extracellular localization of the protein (Fig. 7, *D1* and *E1*). In contrast, CAIV, when injected as purified protein, missing the GPI anchor, could only be detected when the oocytes were permeabilized with methanol and treated with

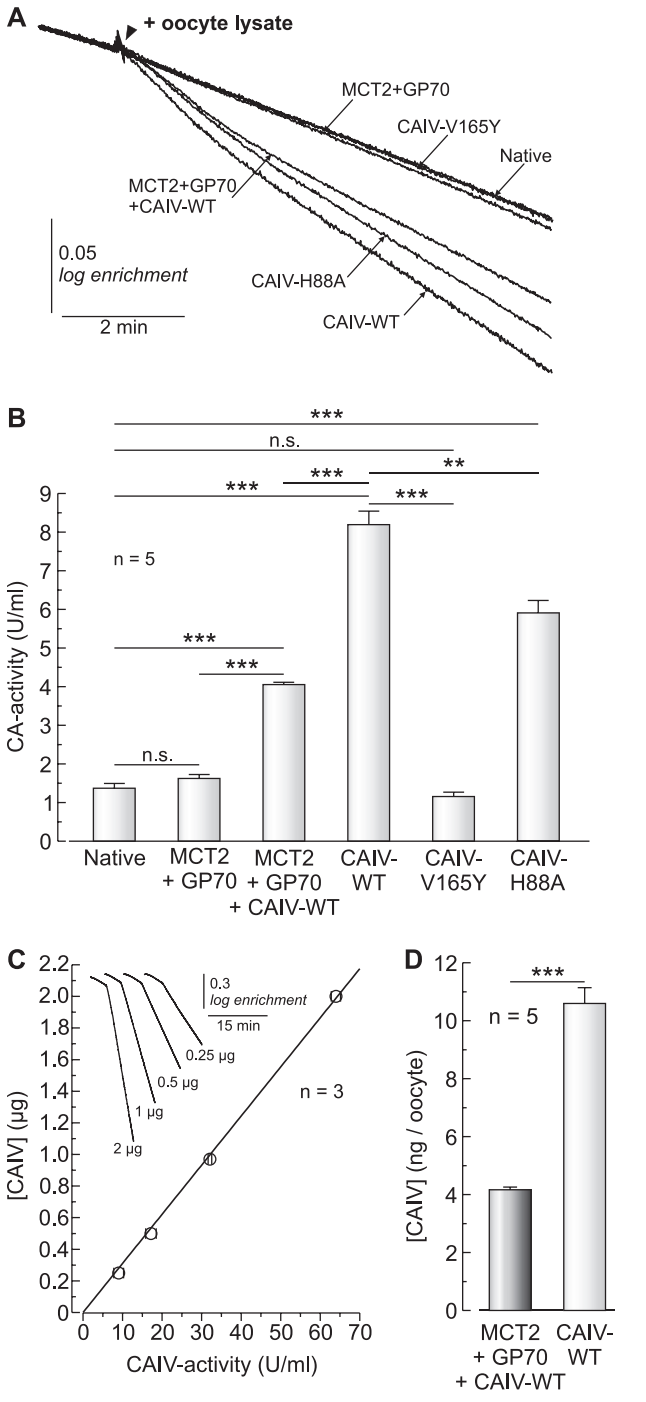

FIGURE 6. **Determination of CA catalytic activity of via mass spectrometry.** *A*, original recordings of the log enrichment of 20 native oocytes and 20 oocytes expressing either MCT2+GP70, MCT2+GP70+CAIV-WT, CAIV-WT, CAIV-H88A, or CAIV-V165Y, respectively. The beginning of the traces shows the rate of degradation of the ^{18}O-labeled substrate in the non-catalyzed reaction. The *black arrowhead* indicates the addition of the oocytes. *B*, enzymatic activity in units/ml at pH 7.0. One unit is defined as 100% stimulation of the non-catalyzed ^{18}O depletion of doubly labeled $^{13}C^{18}O_2$. The *asterisks* above the bars refer to the values of native cells. *C*, calibration curve for the determination of the active CAIV concentration in the oocytes by measuring the activity of different amounts of CAIV protein (0.25, 0.5, 1, and 2 μg) and fitted by linear regression to calculate the amount of expressed CAIV. The *inset* shows the original recordings of the log enrichment for the four amounts of purified CAIV. *D*, amount of CAIV in ng/oocyte in oocytes expressing CAIV-WT alone and in oocytes coexpressing MCT2+GP70+CAIV-WT. A significance level of $p < 0.01$ is marked with **, and $p < 0.001$ with ***.

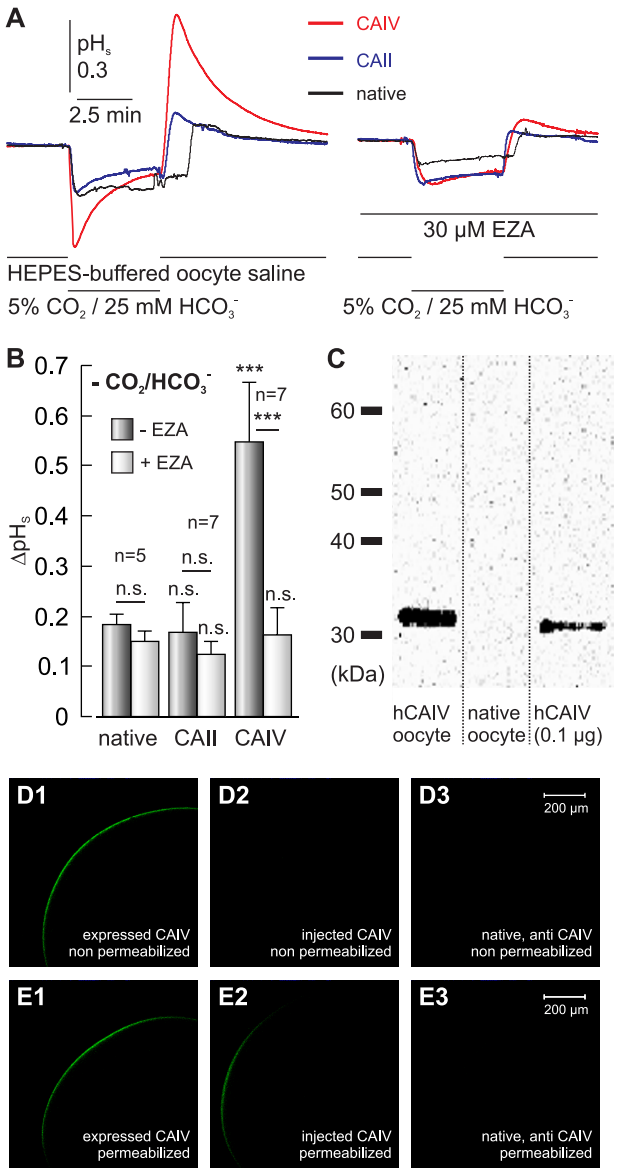

FIGURE 7. **Heterologously expressed CAIV is located at the extracellular surface of the *Xenopus* oocyte.** *A*, original recordings of pH_s at the outer surface of native (*black trace*), CAII-expressing (*blue trace*), and CAIV-expressing (*red trace*) oocytes during application of 5% CO_2/25 mM HCO_3^-, in the absence and presence of 30 μM EZA. *B*, amplitude of the pH_s-transient of native, CAII-expressing, and CAIV-expressing oocytes, as induced by withdrawal of 5% CO_2/25 mM HCO_3^-, in the absence and presence of 30 μM EZA. *C*, Western blot analysis for CAIV from biotinylated native or CAIV-expressing oocytes and of 0.1 μg CAIV protein. Antibody staining against CAIV in oocytes either expressing CAIV (*D1* and *E1*), injected with CAIV protein (*D2* and *E2*), and native oocytes (*D3* and *E3*), respectively, which were either permeabilized with methanol (*E1–3*) or left non-permeabilized (*D1–3*). A significance level of $p < 0.001$ is marked with ***.

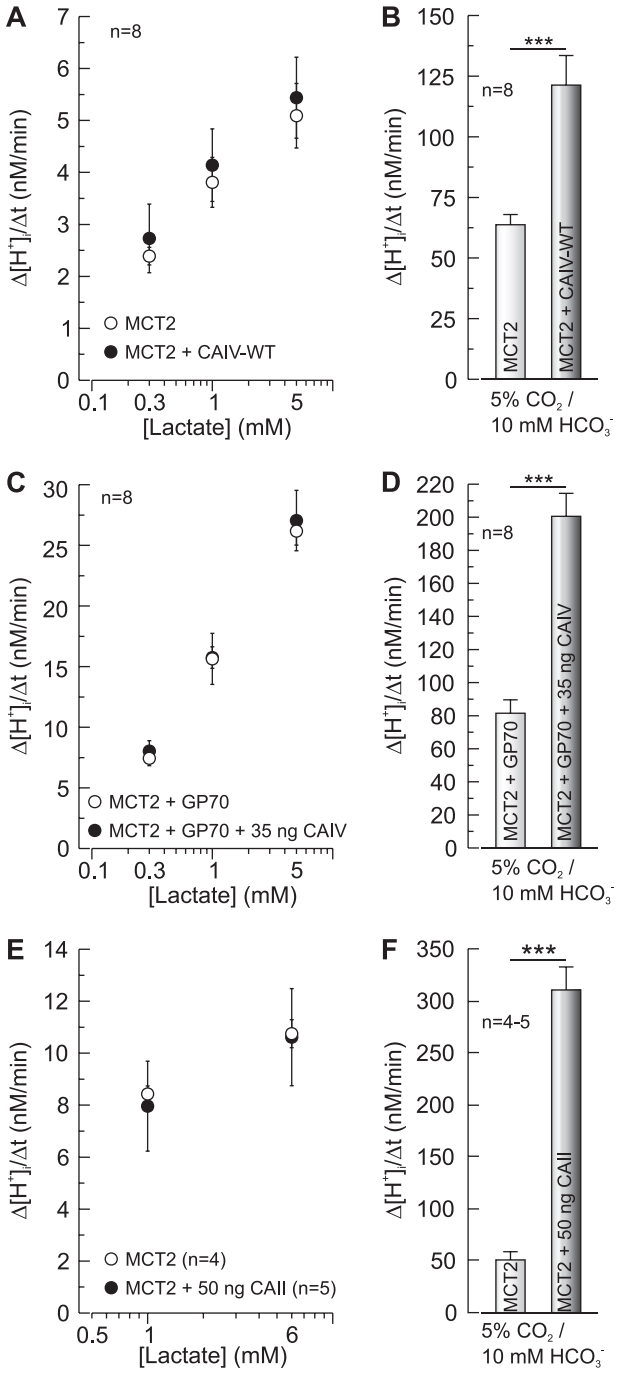

FIGURE 8. **Rate of rise in $[H^+]_i$ as induced by application of 0. 3, 1, and 5 mM lactate (*A, C,* and *E*) and 5% CO_2/10 mM HCO_3^- (*B, D,* and *F*) in oocytes expressing MCT2 or MCT2+CAIV (*A* and *B*), in MCT2+GP70-coexpressing oocytes either injected with 35 ng CAIV protein or H_2O as control (*C* and *D*), and in MCT2-expressing oocytes either injected with 50 ng CAII protein or H_2O as control (*E* and *F*). A significance level of $p < 0.001$ is marked with ***.**

detergents (Fig. 7, *D2* and *E2*). Native control oocytes showed no signal for CAIV at all (Fig. 7, *D3* and *E3*).

GP70 Is Required for CAIV-mediated Increase in MCT2 Transport Activity—To test whether GP70 is necessary for the CAIV-mediated increase in MCT2 transport activity, we coexpressed MCT2 and CAIV without GP70 (Fig. 8, *A* and *B*). Interestingly, CAIV was not able to increase the low MCT2 transport activity in the absence of GP70 (Fig. 8*A*), although CAIV showed full catalytic activity, as determined from the rate of CO_2-induced acidification (*B*). Furthermore, injection of 35 ng of purified CAIV protein, with the GPI anchor removed during purification, showed robust intracellular catalytic activity but did not increase transport activity of MCT2 coexpressed with GP70 (Fig. 8, *C* and *D*). We also injected 50 ng of CAII into just MCT2-expressing oocytes, which displayed high catalytic activity but was again not able to enhance transport activity of MCT2 (Fig. 8, *E* and *F*).

DISCUSSION

Molecular events underlying the regulation of MCT are poorly understood. However, it was recently demonstrated that MCTs require association with an ancillary protein to enable plasma membrane expression and activity. For MCT1, MCT3, and MCT4, the preferred associated protein has been found to be CD147, whereas the preferred ancillary protein for MCT2 is GP70 (9, 10, 41, 42). Furthermore, studies indicate that these chaperones, both glycoproteins containing a single transmembrane domain with a short C terminus located in the cytosol and immunoglobulin-like domains in the extracellular region (43), remain tightly associated with the transporter in the membrane and are also involved in regulation/modulation of inhibitor sensitivity (9, 10, 41, 42, 44). In *X. laevis* oocytes, CD147 is endogenously expressed, whereas GP70, the preferred ancillary protein of MCT2, is not (9). These observations are confirmed by our experiments. Expression of MCT2 without additional GP70 resulted in rather moderate transport activity. In contrast, activity of MCT2 increased about 3- to 5-fold when coexpressed with exogenous GP70 (Fig. 1, *A–C*). The modest activity of MCT2 in the absence of exogenous GP70 is likely to reflect its association with endogenous CD147 because knockdown of intrinsic *X. laevis* CD147 lead to nearly complete abolishment of lactate transport (9). However, we cannot exclude association of MCT2 with another, yet unidentified, intrinsic, ancillary protein.

Furthermore, our data show that the increase in MCT2 activity seems to be based on two factors. The first is increased plasma membrane expression of MCT2 when coexpressed with GP70, accompanied by a reduction of MCT2 beneath the plasma membrane (Fig. 1*D*). The second is an increase in total MCT2 protein level, which is also significantly increased in the presence of GP70 as compared with the situation without GP70 (Fig. 5). Whether the observed difference in MCT2 protein levels are in fact attributable to higher expression or to fast degradation of MCT2 protein not yet inserted, as observed when GP70 is missing, has to be clarified in future experiments.

We have shown previously that CAII can increase the transport activity of MCT1 and MCT4, heterologously expressed in *Xenopus* oocytes, by a mechanism independent of the catalytic activity of the enzyme (22–26). Both in the absence and in the presence of CO_2/ HCO_3^-, blocking CAII catalytic activity with EZA or mutating of the catalytic center of the enzyme (CAII-V143Y) had no effect on the CAII-induced augmentation of MCT1 and MCT4 transport activity (22–24). In contrast, removing the intramolecular H^+ shuttle of CAII (CAII-H64A) or the histidine-rich cluster within the N-terminal of the enzyme (CAII-HEX), which has been suggested to act as a binding site for different acid/base transporters (45), both lead to a loss of interaction between CAII and MCT1/MCT4 (24–25). From this it was concluded that CAII, directly bound to the transporter, can act as an "H^+-collecting antenna" that directly supplies substrate to MCT1 and MCT4 to support proton/lactate cotransport.

In this study, we have now tested for an interaction between CAII and MCT2. Interestingly, CAII did not increase transport activity of MCT2, neither alone nor when GP70 was coexpressed in oocytes. Previous studies have suggested that the interaction between CAII and MCT1 is mediated via the C-terminal of the transporter (22). For the chloride/bicarbonate exchanger AE1, it has been suggested that binding to CAII is mediated via an acidic amino acid cluster (D^{887}ADD) (18). Such acidic clusters can be found in the C-terminal of MCT1 and MCT4 but are absent in the C-terminal of MCT2. Thus, it can be speculated that the interaction between MCT1 and MCT4 and CAII might be mediated by binding of CAII to an acidic cluster within the C-terminal of the two transporters and that no binding of CAII to MCT2 can occur because MCT2 lacks such a cluster. Alternatively, the interaction between MCT and CAII could be mediated or influenced by the ancillary proteins of MCTs. It has been shown, that MCT1 and 4 primarily interact with CD147, which is natively expressed in *Xenopus* oocytes, whereas MCT2 prefers GP70 as an interaction partner. Therefore, it might also be possible that the interaction between CAII and MCTs is mediated by CD147 but not by GP70, leading to an augmentation of activity of MCT1 and 4 but not of MCT2. Therefore, it could be assumed that direct binding between CAII and the transporter is mandatory for initiation of the proton shuttle as described for CAII and MCT1/MCT4.

Our studies showed, however, that transport activity of MCT2 is increased by coexpression with CAIV. The interaction requires CAIV to be localized on the extracellular surface of the oocyte, as injection of CAIV protein has no effect on MCT2-transport activity. In addition, this interaction requires MCT2 to be coexpressed with GP70 because the low transport activity of MCT2 expressed without GP70 was unaffected by CAIV. As already reported for the interaction of MCT1 and MCT4 with CAII (22–26), the CAIV-induced augmentation of MCT2 transport activity does not depend on the catalytic activity of the enzyme. Coexpression of CAIV resulted in an increase in MCT2 transport activity, both in the nominal absence of CO_2/ HCO_3^- and in the presence of the CA inhibitor EZA. The deprotonated sulfonamide group of EZA forms a hydrogen bond with the zinc ion at the catalytic site of CAII but does not interact with the histidine at position 64, the central residue of the CAII intramolecular H^+ pathway (46). Therefore, it appears likely that EZA inhibits CAII catalytic activity but not the intramolecular H^+ shuttle. Furthermore, coexpression of the catalytically inactive mutant CAIV-V165Y resulted in the same augmentation of MCT2 activity as coexpression of MCT2 with CAIV-WT.

We have recently shown that CAII-induced augmentation of MCT1 and MCT4 activity is mediated by the intramolecular proton shuttle of CAII, with His64 as the central part (25). A proton shuttle that moves H^+ between the zinc-bound water and the solvent surrounding the enzyme is also found in CAIV with a histidine residue at position 88 as the central residue. Removal of the intramolecular proton shuttle of CAIV at position 88, by replacing His-88 with Ala, caused a significantly smaller increase in MCT2 activity as compared with wild-type CAIV but, in contrast to the interaction of MCT1 and MCT4 with CAII, did not result in a complete loss of interaction. It has been proposed that CAIV might possess a second, yet unidentified, proton shuttle (47). This second proton shuttle in CAIV

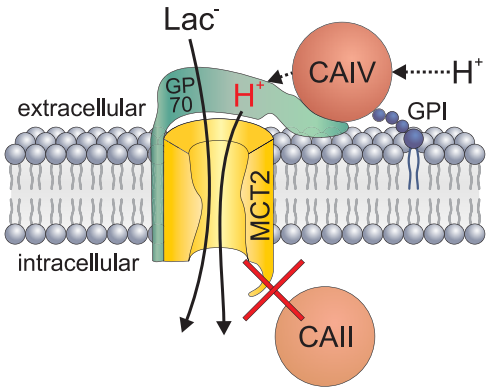

FIGURE 9. **Hypothetical model of the interaction between MCT2 and CAIV.** CAIV (*red circle*), anchored to the extracellular side of the plasma membrane by GPI (*dark blue structure*) is located close to the MCT2 (*yellow structure*) by direct interaction with GP70 (*green*). In this position, CAIV can apply its intramolecular H^+ shuttle to supply H^+ to the MCT2. In contrast, CAII (*orange circle*) does not interact with MCT2, possibly because of a lack of a CAII-binding site in the C-terminal of MCT2, which prevents CAII from getting close enough to the transporter to establish an efficient H^+ shuttle.

might also contribute to the augmented MCT2 transport activity in the presence of CAIV-H88A.

CAIV-induced augmentation of MCT2 transport activity requires coexpression with GP70. It could be speculated that coexpression of CAIV increases the expression level of MCT2. Quantification of the MCT2 expression level in oocytes, however, showed no changes following coexpression with CAIV. Therefore, it can be hypothesized that MCT2 and CAIV may not interact directly with each other but may require GP70 as a mediator, possibly by allowing binding of CAIV to the immunoglobulin-like domains in the extracellular region of the GP70 (Fig. 9). Wherever CAIV might bind, a close approximation to MCT2 appears to be necessary to provide protons for the cotransport with lactate. It has been calculated that H^+ cotransporters like MCTs, whose substrate is only available at very low concentrations, remove H^+ faster from the surrounding aqueous phase than H^+ can diffuse to the transporter, which would lead to depletion of the immediate vicinity of the transporter and would impair transport activity. Therefore, the transporter must exchange H^+ with protonatable sites present in membrane proteins and lipids at the plasma membrane, which need to be located in close proximity to act as a H^+-collecting antenna for the transporter (48). We have recently proposed that intracellular CAII, by facilitating its intramolecular proton shuttle, can act as a proton-collecting antenna for MCT1 and MCT4 to ensure rapid shuttling of lactate and H^+ via the transporters. Similarly, as in the cytoplasm, diffusion of ions in the extracellular space is restricted. For the brain, where MCT2 and CAIV are coexpressed in some types of neurons (16), it has been shown, that extracellular diffusion of ions is hindered by tortuosity of the extracellular space, proteoglycans at the outer membrane surface, charges at the extracellular matrix, but also by extracellular buffers (49, 50). Therefore it appears likely that an effective cotransport of lactate and H^+ across the cell membrane does require proton handling on both sides of the plasma membrane. Because we have demonstrated that extracellular CAIV can enhance transport activity of MCT2 in a non-catalytic manner, CAIV may also act as an extracellular proton-collecting antenna for the MCT2 to facilitate the uptake of lactate and protons from the ECS into active neurons, which have a large demand for energetic substrates.

Acknowledgment—We thank Hans-Peter Schneider for excellent technical assistance.

REFERENCES

1. Halestrap, A. P., and Meredith, D. (2004) *Pflügers Arch.* **447,** 619–628
2. Bröer, S., Bröer, A., Schneider, H. P., Stegen, C., Halestrap, A. P., and Deitmer, J. W. (1999) *Biochem. J.* **341,** 529–535
3. Garcia, C. K., Brown, M. S., Pathak, R. K., and Goldstein, J. L. (1995) *J. Biol. Chem.* **270,** 1843–1849
4. Jackson, V. N., Price, N. T., Carpenter, L., and Halestrap, A. P. (1997) *Biochem. J.* **324,** 447–453
5. Halestrap, A. P., and Price, N. T. (1999) *Biochem. J.* **343,** 281–299
6. Bergersen, L., Waerhaug, O., Helm, J., Thomas, M., Laake, P., Davies, A. J., Wilson, M. C., Halestrap, A. P., and Ottersen, O. P. (2001) *Exp. Brain. Res.* **136,** 523–534
7. Pellerin, L., Pellegri, G., Bittar, P. G., Charnay, Y., Bouras, C., Martin, J. L., Stella, N., and Magistretti, P. J. (1998) *Dev. Neurosci.* **20,** 291–299
8. Pierre, K., and Pellerin, L. (2005) *J. Neurochem.* **94,** 1–14
9. Ovens, M. J., Manoharan, C., Wilson, M. C., Murray, C. M., and Halestrap, A. P. (2010) *Biochem. J.* **431,** 217–225
10. Wilson, M. C., Meredith, D., Fox, J. E., Manoharan, C., Davies, A. J., and Halestrap, A. P. (2005) *J. Biol. Chem.* **280,** 27213–27221
11. Supuran, C. T., and Scozzafava, A. (2007) *Bioorg. Med. Chem.* **15,** 4336–4350
12. Supuran, C. T. (2009) *Drug Design of Zinc-Enzyme Inhibitors*, pp. 15–16, John Wiley & Sons, Inc., Hoboken, New Jersey
13. Cammer, W. (1979) *J. Neurochem.* **32,** 651–654
14. Deitmer, J. W., and Rose, C. R. (1996) *Prog. Neurobiol.* **48,** 73–103
15. Svichar, N., Esquenazi, S., Waheed, A., Sly, W. S., and Chesler, M. (2006) *Glia* **53,** 241–247
16. Svichar, N., and Chesler, M. (2003) *Glia* **41,** 415–419
17. McMurtrie, H. L., Cleary, H. J., Alvarez, B. V., Loiselle, F. B., Sterling, D., Morgan, P. E., Johnson, D. E., and Casey, J. R. (2004) *J. Enzyme. Inhib. Med. Chem.* **19,** 231–236
18. Vince, J. W., and Reithmeier, R. A. (1998) *J. Biol. Chem.* **273,** 28430–28437
19. Becker, H. M., and Deitmer, J. W. (2007) *J. Biol. Chem.* **282,** 13508–13521
20. Pushkin, A., Abuladze, N., Gross, E., Newman, D., Tatishchev, S., Lee, I., Fedotoff, O., Bondar, G., Azimov, R., Ngyuen, M., and Kurtz, I. (2004) *J. Physiol.* **559,** 55–65
21. Li, X., Alvarez, B., Casey, J. R., Reithmeier, R. A., and Fliegel, L. (2002) *J. Biol. Chem.* **277,** 36085–36091
22. Becker, H. M., Hirnet, D., Fecher-Trost, C., Sültemeyer, D., and Deitmer, J. W. (2005) *J. Biol. Chem.* **280,** 39882–39889
23. Becker, H. M., and Deitmer, J. W. (2008) *J. Biol. Chem.* **283,** 21655–21667
24. Becker, H. M., Klier, M., and Deitmer, J. W. (2010) *J. Membr. Biol.* **234,** 125–135
25. Becker, H. M., Klier, M., Schüler, C., McKenna, R., and Deitmer, J. W. (2011) *Proc. Natl. Acad. Sci. U.S.A.* **108,** 3071–3076
26. Almquist, J., Lang, P., Prätzel-Wolters, D., Deitmer, J. W., Jirstrand, M., and Becker, H. M. (2010) *J. Comput. Sci. Syst. Biol.* **3,** 107–116
27. Juel, C., Lundby, C., Sander, M., Calbet, J. A., and Hall, G. (2003) *J. Physiol.* **548,** 639–648
28. Alvarez, B. V., Loiselle, F. B., Supuran, C. T., Schwartz, G. J., and Casey, J. R. (2003) *Biochemistry* **42,** 12321–12329
29. Sterling, D., Alvarez, B. V., and Casey, J. R. (2002) *J. Biol. Chem.* **277,** 25239–25246
30. Wetzel, P., Hasse, A., Papadopoulos, S., Voipio, J., Kaila, K., and Gros, G. (2001) *J. Physiol.* **531,** 743–756
31. Messonnier, L., Kristensen, M., Juel, C., and Denis, C. (2007) *J. Appl. Physiol.* **102,** 1936–1944
32. Hallerdei, J., Scheibe, R. J., Parkkila, S., Waheed, A., Sly, W. S., Gros, G., Wetzel, P., and Endeward, V. (2010) *PLoS ONE* **5,** e15137

33. Becker, H. M., Bröer, S., and Deitmer, J. W. (2004) *Biophys. J.* **86,** 235–247
34. Silverman, D. N. (1982) *Methods Enzymol.* **87,** 732–752
35. Sültemeyer, D. F., Fock, H. P., and Canvin, D. T. (1990) *Plant Physiol.* **94,** 1250–1257
36. Badger, M. R., and Price, G. D. (1989) *Plant Physiol.* **89,** 51–60
37. Deitmer, J. W. (1991) *J. Gen. Physiol.* **98,** 637–655
38. Bröer, S., Schneider, H. P., Bröer, A., Rahman, B., Hamprecht, B., and Deitmer, J. W. (1998) *Biochem. J.* **333,** 167–174
39. Vaughan-Jones, R. D., and Spitzer, K. W. (2002) *Biochem. Cell Biol.* **80,** 579–596
40. Ro, H. A., and Carson, J. H. (2004) *J. Biol. Chem.* **279,** 37115–37123
41. Kirk, P., Wilson, M. C., Heddle, C., Brown, M. H., Barclay, A. N., and Halestrap, A. P. (2000) *EMBO J.* **19,** 3896–3904
42. Wilson, M. C., Meredith, D., and Halestrap, A. P. (2002) *J. Biol. Chem.* **277,** 3666–3672
43. Fossum, S., Mallett, S., and Barclay, A. N. (1991) *Eur. J. Immunol.* **21,** 671–679
44. Wilson, M. C., Meredith, D., Bunnun, C., Sessions, R. B., and Halestrap, A. P. (2009) *J. Biol. Chem.* **284,** 20011–20021
45. Vince, J. W., Carlsson, U., and Reithmeier, R. A. (2000) *Biochemistry* **39,** 13344–13349
46. Di Fiore, A., Pedone, C., Antel, J., Waldeck, H., Witte, A., Wurl, M., Scozzafava, A., Supuran, C. T., and De Simone, G. (2008) *Bioorg. Med. Chem. Lett.* **18,** 2669–2674
47. Hurt, J. D., Tu, C., Laipis, P. J., and Silverman, D. N. (1997) *J. Biol. Chem.* **272,** 13512–13518
48. Bolaños, J. P., and Heales, S. J. (2010) *Front. Neuroenergetics* **2,** 1–8
49. Syková, E., and Nicholson, C. (2008) *Physiol. Rev.* **88,** 1277–1340
50. Voipio, J., and Ballanyi, K. (1997) *J. Physiol.* **499,** 527–542